

Exploration of iron ligand modes in dimeric iron (II) complexes by nuclear resonance scattering

Andreas Omlor¹ · Sergej Lauk² · Christina Sophia Müller¹ · Lena Scherthan¹ · Hendrik Auerbach¹ · Tim Hochdörffer¹ · Juliusz A. Wolny¹ · Rene Steinbrügge³ · Olaf Leupold³ · Ilya Sergeev³ · Hans Christian Wille³ · Helmut Sitzmann² · Volker Schünemann¹

Published online: 10 February 2020
© Springer Nature Switzerland AG 2020

Abstract

The vibronic properties of two dimeric iron (II) high-spin complexes [⁵CpFeX]₂ (⁵Cp = Pentaïso-propyl-cyclopentadienyl, X = OH-(1), Br-(2)) have been studied using nuclear inelastic scattering (NIS). In order to assign the experimentally observed bands to the particular modes, theoretical calculations using density functional theory (DFT) have been performed based on the structural data obtained by X-ray crystallography. The calculated partial density of vibrational states (pDOS) reproduces the experimental data. Thus, we were able to assign almost each of the experimentally observed NIS bands to their corresponding molecular vibrational modes.

Keywords Nuclear inelastic scattering · Ferrocenes · Iron (II) high-spin complexes · Density functional theory calculations

This article is part of the Topical Collection on *Proceedings of the International Conference on the Applications of the Mössbauer Effect (ICAME2019), 1-6 September 2019, Dalian, China*
Edited by Tao Zhang, Junhu Wang and Xiaodong Wang

Electronic supplementary material The online version of this article (<https://doi.org/10.1007/s10751-019-1663-y>) contains supplementary material, which is available to authorized users.

✉ Andreas Omlor
omlor@rhrk.uni-kl.de

¹ Department of Physics, Technische Universität Kaiserslautern, Erwin-Schrödinger-Straße 56, 67663 Kaiserslautern, Germany

² Department of Chemistry, Technische Universität Kaiserslautern, Erwin-Schrödinger-Straße 52, 67663 Kaiserslautern, Germany

³ Petra III P01, DESY, Notkestraße 85, 22607 Hamburg, Germany

1 Introduction

Ferrocene has been investigated at the beginning of the 1950's [1]. Since that time a variety of applications of ferrocene derivatives were developed e.g. for the preparation of iron containing nanotubes, for vapor-phase insertion of ferrocenes into zeolites or even in luminescent systems for the intramolecular quenching of excited singlet states [2–4]. Also in catalysis, most common in chiral catalysis with asymmetrically substituted ferrocenes [5], ferrocene derivatives are important. We have studied two different Fe^{II} containing complexes to investigate such catalysts. Both complexes are feasible as starting compounds for a catalytic dehydrogenative P-P coupling reaction [6]. The dimeric structure $[\text{}^5\text{CpFeX}]_2$ consists of two iron cyclopentadienyl units ($\text{}^5\text{Cp}$ = Penta-isopropylcyclopentadienyl, $\text{X} = \text{Br}^-$, OH^-) bridged over two bromine or hydroxide ions. The investigation of the vibrational properties of iron (II) high-spin complexes is of interest as they are of general importance for the iron-ligand bond strength which may influence the catalytic performance of these systems in homogenous catalysis. For that purpose, we have applied nuclear inelastic scattering (NIS) to investigate the vibrational properties of these complexes.

2 Materials and methods

The $[\text{}^5\text{CpFeX}]_2$ complexes under study $\text{C}_{40}\text{H}_{70}\text{Br}_2\text{Fe}_2$ **1** and $\text{C}_{40}\text{H}_{72}\text{O}_2\text{Fe}_2$ **2** were prepared at the Technische Universität Kaiserslautern. Details of the preparation will be published separately. A structural view of both complexes is given in Figs. 1 and 2. The structural views are

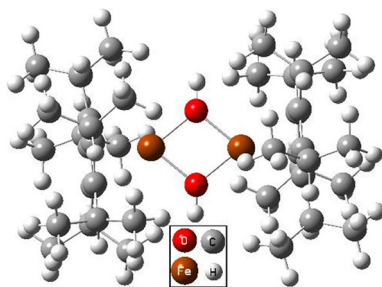


Fig. 1 Structural view of **1** obtained by X-ray crystallography and subsequent optimization with Gaussian 16 (B3LYP/CEP31-g)

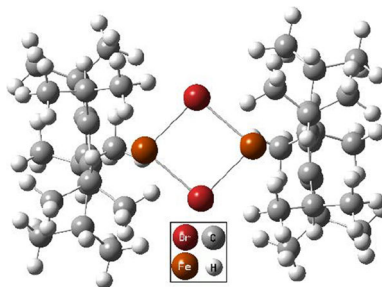


Fig. 2 Structural view of **2** obtained by X-ray crystallography and subsequent optimization with Gaussian 16 (B3LYP/CEP31-g)

based on a preliminary X-ray single crystal analysis and subsequent energy minimization using density functional theory (DFT) as described below. The NIS experiments were carried out at the “High Resolution Dynamics Beamline P01” at Petra III, DESY in Hamburg, Germany under experiment No. 11005163. The operation of the storage ring was a 40-bunch mode (bunch separation of 192 ns) with a beam energy of 6 GeV. The experimental setup established at the beamline including a two-step monochromatization (energy resolution of ~ 1 meV) and detection by avalanche photo diodes was used. Cooling of the powder samples to $T = 4.2$ K was reached by a dedicated cryostat from Janis Research. The NIS data were collected during several scans within the energy range of -20 to 80 meV with a 0.25 meV step size and a measuring time of 5 s per energy step. The experimentally determined partial density of vibrational states (pDOS) was calculated with a binning of 0.5 meV. The theoretically calculated pDOS results from DFT calculations including normal mode calculations by means of Gaussian16 Rev. A.03 [7]. With the structural data from X-ray crystallography as input, energy minimization was achieved using the B3LYP functional and the CEP-31G basis set. All calculations were carried out under the assumption that the $S = 2$ spins of the individual high-spin iron(II) centers are coupled parallel to a total spin of $S_T = 4$. This assumption is based on measurements on structurally very similar systems [8].

3 Results and discussion

The experimentally determined pDOS of **1** obtained at $T = 4.2$ K (see Fig. 3a) shows five distinct areas (I to V) (marked with different colors in Figs. 3 and 4, and in text with roman numbers from I to V) with peak maxima at $92(\text{I})$, $124(\text{I})$, $157(\text{II})$, $177(\text{II})$, $237(\text{III})$, $281(\text{III})$, $398(\text{IV})$, $418(\text{IV})$, $455(\text{IV})$, $503(\text{IV})$ and $535(\text{V})$ cm^{-1} . The corresponding simulation of the NIS data based on DFT calculations and the subsequent normal mode analysis with Gaussian 16 is shown in Fig. 3b. The vertical lines in the simulation illustrate the mode compensation factor of the iron atoms as a function of the vibrational energy of the corresponding vibrations. The calculated modes at 80 and 88 cm^{-1} coincide with the experimentally obtained band at 92 cm^{-1} . Similarly, the two modes at 104 and 116 cm^{-1} of the simulation collapse together to form a band at 124 cm^{-1} in the measured spectrum. The calculated modes at 172 cm^{-1} and 192 cm^{-1} are also observable in the experimental data as separate bands at 157 and 177 cm^{-1} respectively. The two bands present in region III can be found both in the measured spectrum (237 cm^{-1} and 281 cm^{-1}) and in the simulation (228 cm^{-1} and 284 cm^{-1}). In section IV there are three bands which can be assigned to intensive Fe-OH oscillations. These are clearly visible in the simulation as well as in the measured spectrum. The last two bands in the spectrum (499 cm^{-1} and 535 cm^{-1}) are in reasonable agreement to the calculated modes (488 and 528 cm^{-1}).

Also the experimentally determined pDOS of the bromine bridged complex **2** (see Fig. 4a) can be divided in five main parts with the peak maxima at $80(\text{I})$, $116(\text{I})$, $149(\text{II})$, $201(\text{II})$, $266(\text{III})$, $282(\text{III})$, $496(\text{V})$ and $504(\text{V})$ cm^{-1} . The pDOS of this complex lacks vibrational bands in area IV. The shape of the two bands in region I is slightly different from the simulation. However, the low-energy part of the experimental pDOS (peaks at 80 and 116 cm^{-1}) is only poorly reproduced by the DFT calculations. In this area (< 100 cm^{-1}) the simulation consists of several intensive modes, indicated by the six vertical lines which show the displacement of the iron atoms. This fact complicates the prediction of the exact shape of the bands. It is possible for single modes to overlap and lead to the measured spectrum. Taking a closer look at the

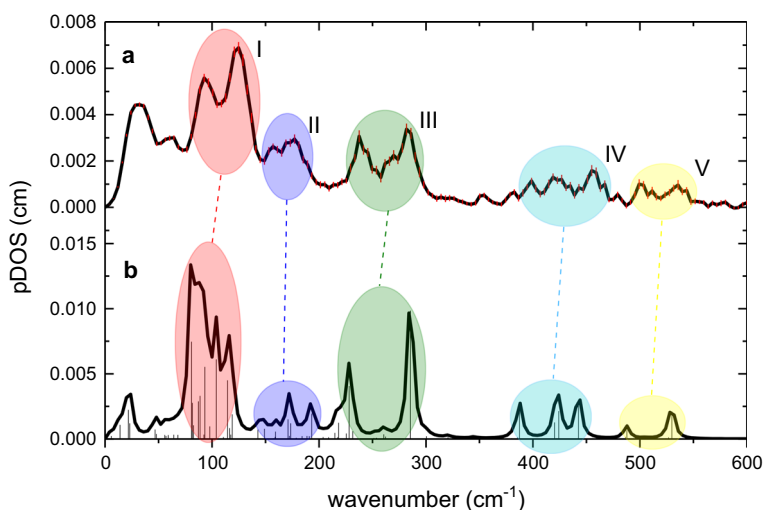


Fig. 3 **a** Experimental pDOS of **1** determined from NIS obtained at 4.2 K; **b** DFT calculated pDOS of **1** based on the structure given in Fig. 1

further simulation, shows vibrations at higher wavenumbers which occur more separately, what allows a more accurate prediction of the spectrum. For this reason, the simulation of the regions II to V fits very well to the measured spectrum.

Both pDOS show characteristic bands in the area of 100 to 300 cm^{-1} , typical for Fe^{II} high-spin systems [9]. In order to be able to compare more easily the vibrations with each other, a unified surface for both complexes is defined relative to which the vibrations are described. This surface is spanned by four atoms situated in a plane. These are the two iron atoms and the two bridging ligands (oxygen or bromine). The bands in region I of complex **1** (92 cm^{-1}) and **2** (80 cm^{-1}) correspond amongst others to an intensive iron-iron bending mode (see Fig. 5). The

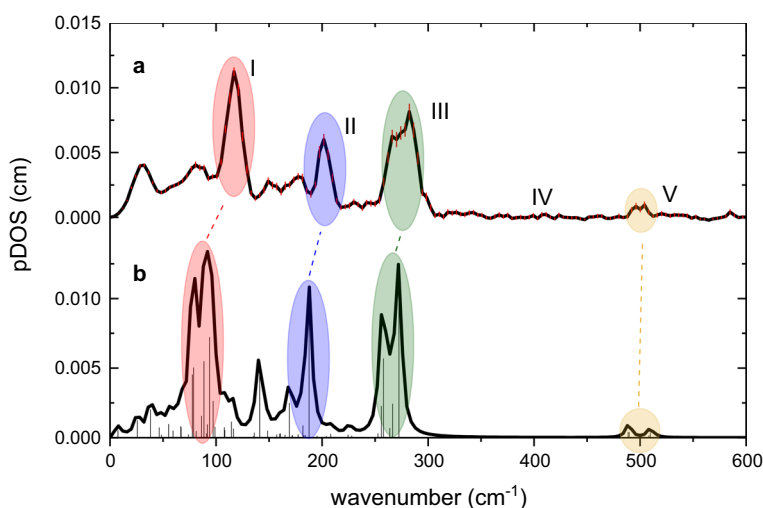


Fig. 4 **a** Experimental pDOS of **2** determined from NIS obtained at 4.2 K; **b** DFT calculated spectrum of **2** based on the structure given in Fig. 2

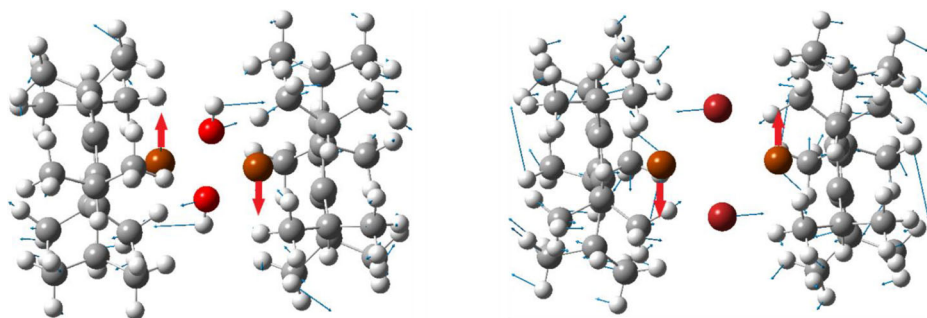


Fig. 5 Representation of characteristic modes in the DFT simulation of **1** (left) at 228 cm^{-1} and **2** (right) at 257 cm^{-1} . The red arrows are located in the moving direction of the iron centers. The blue arrows represent the movements of the ligand atoms

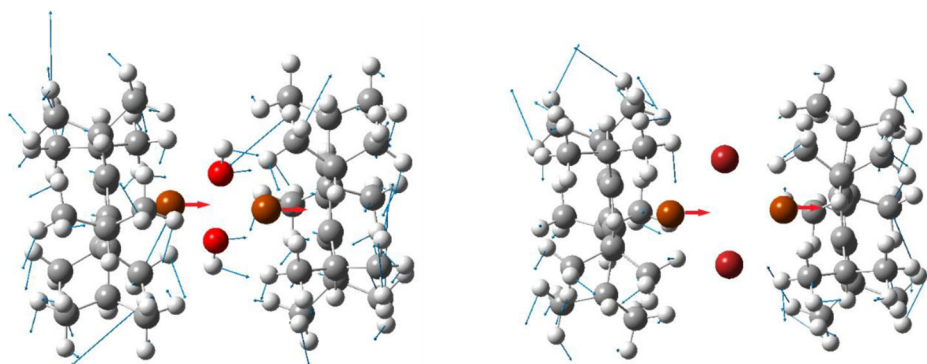


Fig. 6 Characteristic symmetric vibrations at 228 cm^{-1} (left, complex **1**) and 257 cm^{-1} (right, complex **2**)

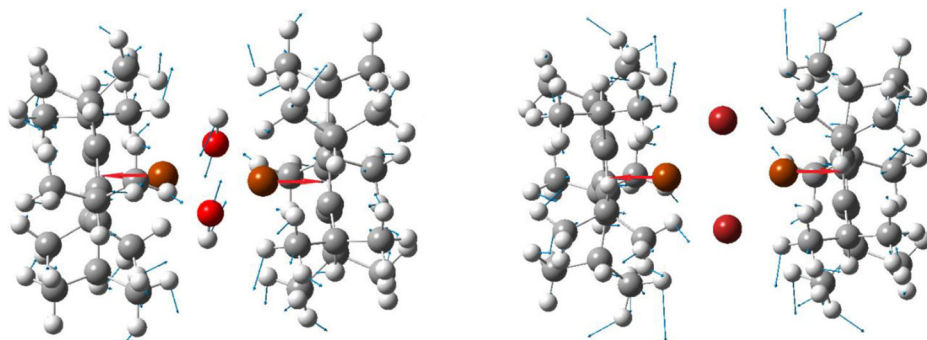


Fig. 7 Characteristic asymmetric vibrations at 285 cm^{-1} (left, complex **1**) and 272 cm^{-1} (right, complex **2**)

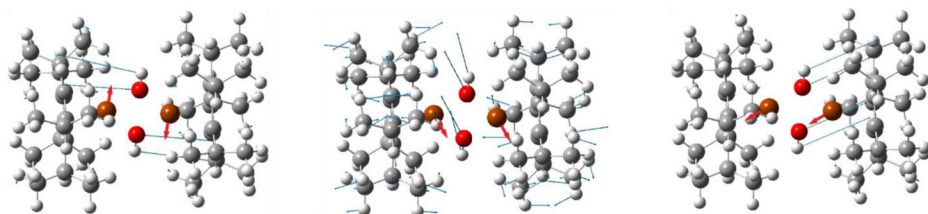


Fig. 8 Three vibrational modes at 387 (left), 424 (middle) and 442 cm^{-1} (right) which only occur at the OH bridged complex **1**

Table 1 Lamb–Mössbauer factor (f_{LM}) and several thermodynamic parameters

Complex	T (K)	f_{LM}	Mean internal energy (meV)	Mean force constant D (N/m)
($^5\text{CpFeOH}$) ₂ 1	4.2	0.84	33.88	3.202
($^5\text{CpFeBr}$) ₂ 2	4.2	0.85	30.19	2.025

iron atoms move perpendicularly to the Fe_2Br_2 or Fe_2O_2 plane. Movies of all mentioned vibrations can be found in the SI.

The modes at 228 cm^{-1} (**1**) and 257 cm^{-1} (**2**) correspond to the same oscillation mode. These are symmetric stretching oscillations parallel to the iron-iron bridging ligand surface (see Fig. 6).

In contrast to both symmetric vibrations there are also very similar asymmetric vibrations in complex **1** and **2**. The asymmetric vibrations are located at 285 cm^{-1} (**1**) and 272 cm^{-1} (**2**). The displacements of the iron atoms are shown in Fig. 7.

In the fourth region, only at complex **1** oscillations occurred. Figure 8 shows the individual oscillations that occurred for the OH-bridged complex. These are asymmetric oscillations (at 387 cm^{-1}) out of the fictive plane as well as symmetric oscillations in the defined plane (at 424 and 442 cm^{-1}).

With this technique we are also able to determine the Lamb–Mössbauer factor (f_{LM}) and several thermodynamic parameters, including the mean internal energy (U), the entropy (S_{vib}), the free enthalpy as well as the normalized mean force constant (D) of the complexes (see Table 1).

The mean force constant D of the OH bridged complex is higher than the value of the Br bridged complex. This behavior was expected because of the shorter Fe–OH bonding.

Acknowledgements This work has been supported by the German Science foundation (DFG) via the SFB-TRR-88 3MET and via the individual grant SI 366/15-1.

References

1. Kealy, T.J., Pauson, P.L.: Nature. **168**, 1039–1040 (1951)
2. Krupskaya, Y., Mahn, C., et al.: J. Magn. Magn. Mater. **321**, 4067–4071 (2009)
3. Moller, K., Borvornwattananont, A., Bein, T.: J. Phys. Chem. **93**, 4562–4571 (1989)
4. Fery-Forgues, S., Delavaux-Nicot, B.: J. Photochem. Photobiol. A Chem. **132**, 137–159 (2000)
5. Atkinson, R.C.J., Gibson, V.C., Long, N.J.: The syntheses and catalytic applications of unsymmetrical ferrocene ligands. Chem. Soc. Rev. **33**, 313–328 (2004)
6. Groß, O.A., Lauk, S., Müller, C., Gidt, W., Sun, Y., Demeshko, S., Meyer, F., Sitzmann, H.: Eur. J. Inorg. Chem. **30**, 3635–3643 (2017)

7. M. Frisch et al., Gaussian 16; Gaussian, Inc.; Revision A.03, Wallingford CT, 2016
8. Sitzmann, H., Dezember, T., et al.: *Angew. Chem. Int. Ed. Eng.* **35**, 2872–2875 (2004)
9. Wolny, J.A., Rackwitz, S., Achterhold, K., Muffler, K., Schünemann, V.: *Hyperfine Interact.* **204**, 129–132 (2012)

Publisher's note Springer Nature remains neutral with regard to jurisdictional claims in published maps and institutional affiliations.